



## Telon Blue AGLF Adsorption by NiO-Based Nanomaterials: Equilibrium, Kinetic, and Thermodynamic Approach

Gizem BİÇER<sup>1</sup> , Ferda GÖNEN<sup>1,a</sup> 

<sup>1</sup>.Mersin University, Department of Chemical Engineering, Mersin, TÜRKİYE

**Abstract:** In this study, the effects of adsorption parameters such as initial pH, initial dye concentration, temperature, and adsorbent dosage on the colour removal from aqueous solution containing Telon Blue AGLF (TB AGLF) textile dye were investigated by NiO-based nanomaterials and then the compliance of the equilibrium data with the different isotherm models in the literature was evaluated. In the next step, the adsorption system was analyzed regarding kinetics and thermodynamics. At the end of the study, XRD, SEM and FTIR analysis methods were used for the particle characterization. As a result of the experimental studies, it was detected the successful use of NiO-based nanomaterials synthesized by aqueous solution method rarely seen in literature for color removal. Through this study, it is believed that the additional contributions are provided to the scientific investigations about the recovery of the water resources.

**Keywords:** NiO nanoparticles, TB AGLF, adsorption.

**Submitted:** April 15, 2017. **Accepted:** June 09, 2017.

**Cite this:** Biçer G, Gönen F. Telon Blue AGLF Adsorption by NiO-Based Nanomaterials: Equilibrium, Kinetic, and Thermodynamic Approach. JOTCSA. 2017 Jun;4(3):675-90.

**DOI:** <http://doi.org/10.18596/jotcsa.291249>.

**\*Corresponding author.** E-mail: [gonenf74@gmail.com](mailto:gonenf74@gmail.com).

## INTRODUCTION

Many harmful organic and inorganic substances such as aromatic compounds, heavy metals, and dyestuffs exist in the content of the wastewater from different industries. The main branches of industries produce colored wastewaters are textiles, leather, printing, laundry, tannery, rubber, plastic, and paint. Wastewaters containing dyestuffs can be noticed easily as well as they may cause reduction of gas solubility and light scattering (1). Also, it is known that the majority of dyestuffs and pigments have harmful effects on human and aquatic life (2).

Due to the adverse effects of dyestuffs on flora and fauna, wastewater containing this pollutant should be necessarily treated before discharging to the receiving environment. Conventional treatment methods for dyestuff-containing wastewater are coagulation, flocculation, ion exchange, membrane processes and oxidation (3). High energy expenses, insufficient pollutant removal efficiency and the formation of different toxic wastes require a new treatment methods are important restrictions that have made these methods unpreferable (4). According to the scientific researches in recent years, it has proved that dyestuffs resist to biologic degradation because of their high molecular weight and some inert materials in their structure (5). When compared to other treatment methods, adsorption is known as a preferable treatment technic from the viewpoint of high removal efficiency and the ease of operation (6). In addition to ease of operation and high color removal yield, the other important advantages of this method are compatibility with the environment and low cost-effectiveness (7). If it is searched the current investigations in the literature, it is seen that highly qualified, different and alternative adsorbents are used for wastewater treatment by adsorption. Various adsorbents (activated carbon, bentonite, clay, silica gel, alumina, banana peel, kaolinite clay, wood, bagasse) have been investigated and used for the removal of dyes from wastewater (8). Some of these adsorbents cannot be widespread used because of their high cost, difficult disposal and regeneration difficulties. In recent years, with the development of nanotechnology, nanoporous and nanostructured materials have been selected as an adsorbent for water treatment processes. These materials exhibit a higher removal capacity for dyes, which has become the focused research area of magnetic separation technology because of their excellent physicochemical characteristics and larger specific surface areas. Especially, metal nanoparticles (NPs) with controlled size and shape are of considerable interest because of their morphology-dependent properties (9) and potential applications in a lot of fields (10). In this study, color removal was investigated from an aqueous solution containing Telon Blue AGLF dye by selective, easily reproducible, inexpensive and green NiO-based nanoparticles because of their excellent physicochemical characteristics and

larger specific surface areas providing high removal capacity for dyes. In addition, the interaction between the adsorbent and the solution was investigated using classical methods, the effects of adsorption variables on color removal from wastewater and the most relevant experimental conditions were determined. At the last stage, adsorption equilibrium, and thermodynamics were investigated, and adsorption mechanism was analyzed by kinetic model equations.

## MATERIALS AND METHODS

### Chemicals

NiSO<sub>4</sub> and Ni(OH)<sub>2</sub> used in nanomaterial synthesis were purchased from Sigma–Aldrich. Also, Telon Blue AGLF dye was purchased from Sigma–Aldrich. Its Molecular Weight [MW]: 735.85; Molecular Formula [MF]: C<sub>37</sub>H<sub>38</sub>N<sub>5</sub>NaO<sub>6</sub>S<sub>2</sub>; λ<sub>max</sub>: 610 nm. The corresponding chemical structure of Telon Blue AGLF dye is depicted in Fig. 1.

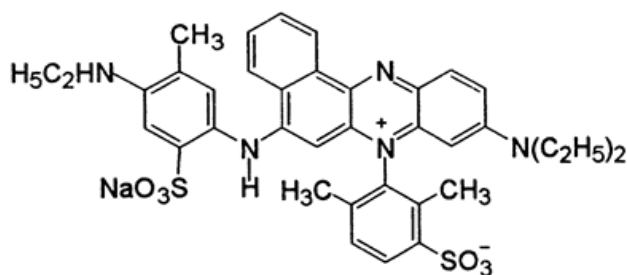


**Figure 1:** The chemical structure of Telon Blue AGLF

Also, the Accurate quantity of the dye in doubly distilled water was dissolved in order to prepare the 1000 mg L<sup>-1</sup> stock solution. The experimental solutions used in experiments were obtained by diluting the stock solution to the desired initial dye concentration.

### NiO-based Nanomaterial Synthesis

In experimental study, removal of colour from synthetic wastewater containing TB AGLF dye was investigated by using the average particle size of 100 nm NiO-based nanomaterials synthesized by aqueous solution method According to this method, 2.0 g of dried NiSO<sub>4</sub> was added to 25 mL of 1 M Nickel hydroxide, at 200 rpm stirrer speed for 1 h. The Ni-diatomite material was separated by filtration. The calcination process was carried out by placing modified diatomite sample in the furnace at 250°C for 4.5 h. The synthesized nanomaterial was then allowed to cool in a desiccator (11).

### **Adsorption Studies**

250 mL erlenmeyer flasks of 150 mL test volume used as the reaction vessels in the adsorption process were placed in shaking water bath at constant stirring speed and temperature, the two phases in the samples taken at specific time intervals following the addition of nanomaterials to the dye solution were separated from each other by centrifugation and then on adsorbed dye concentration remaining in the liquid phase was determined spectrophotometrically at wavelength of 610 nm (12) The molar extinction coefficient of the TB AGLF dye solution was found to be  $10.48 \times 10^3 \text{ mol}^{-1} \text{ L cm}^{-1}$ . In this investigation, the studied concentrations of TB AGLF dyes are 25, 50, 75, 100, 200, 300, 400, 500, 750, 1000, 1500  $\text{mg L}^{-1}$ , and the temperatures of 30, 40, 50, 60  $^{\circ}\text{C}$ . In addition, the removal of TB AGLF by nanomaterial was studied at different adsorbent doses such as 0.50, 1.0, 2.0, 3.0 and 4.0  $\text{g L}^{-1}$ . Adsorption experiments were repeated more than two times to make sure the results.

### **Adsorbent Characterization**

FTIR (Perkin Elmer, Fourier Transform Infrared Spectrometer), SEM (Zeiss / Supra 55 Area Emission, Scanned Electron Microscope), and XRD (Philips, X'Pert brand X-Ray Diffractometer) were used for identification of functional groups belonging to the nanomaterials before and after adsorption, identification of morphological properties and identification of phases and crystal structures, respectively.

## **RESULTS**

### **Change of Adsorbent Structure During Adsorption**

FT-IR(Fourier Infrared Transform Spectroscopy), SEM(Scanning Electron Microscopy) and XRD (X-Ray Diffractometer) analyze of adsorbents were carried out before and after adsorption in order to determine the mechanisms of adsorption of Telon blue AGLF dye to NiO-based nanomaterials and are presented in Figure 2-4. According to FTIR, SEM and XRD spectra, TB AGLF dye loaded NiO-based adsorbent demonstrated either shift or reduction in adsorption peaks proposing the vital role played by the functional groups.

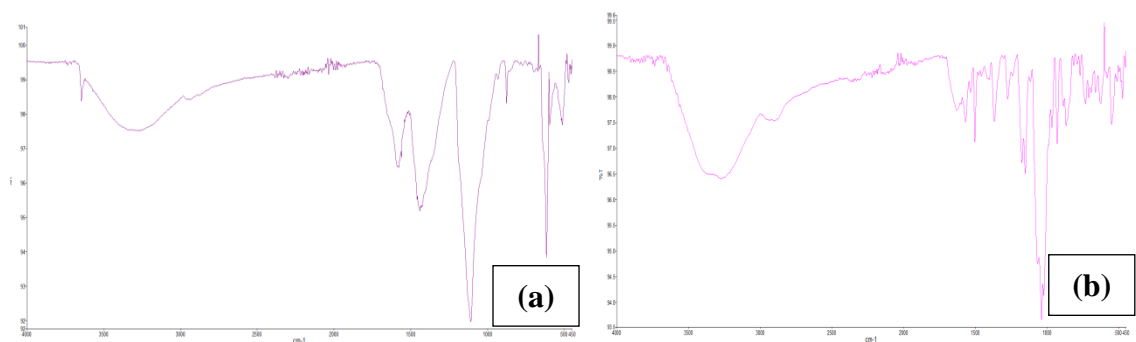


**Figure 2:** FTIR spectra of NiO-based nanomaterials before(a) and after (b) adsorption

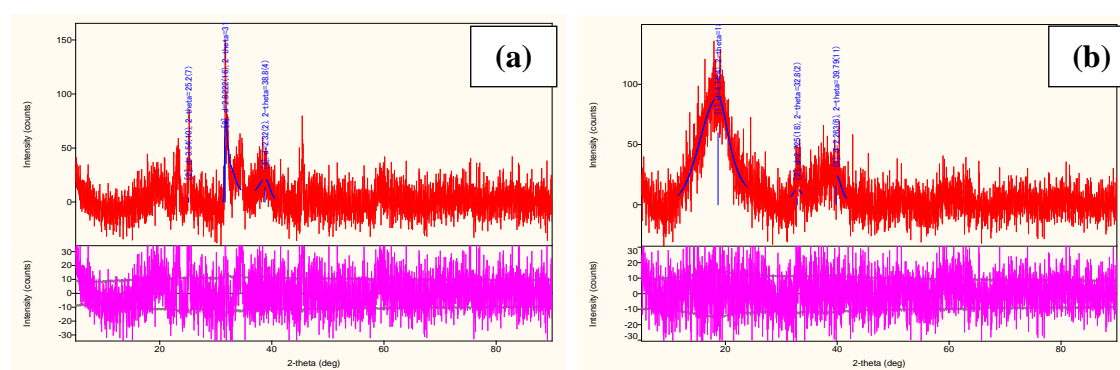


**Figure 3:** XRD spectra of NiO-based nanomaterials before (a) and after (b) adsorption.

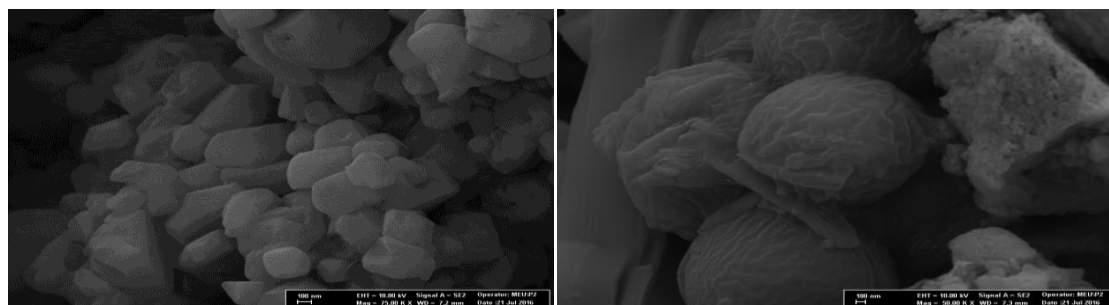


**Figure 4:** SEM images of NiO-based nanomaterials before (a) and after (b) adsorption

FT-IR analyze technique was used to investigate the mechanism of Telon blue AGLF adsorption onto NiO-based nanomaterials, and SEM images of these materials before and after adsorption are presented in Figure 2. From the SEM images, the band at  $3272.34\text{ cm}^{-1}$  illustrates the (OH) atom and the bands at  $1558.28, 1503.13\text{ cm}^{-1}$  illustrate the (H) atom and the peaks at  $1367.35\text{ cm}^{-1}$  and  $1274.16\text{ cm}^{-1}$  are due to the C-C and C-O group stretching, respectively. In addition to this, the bands at  $1151.56, 549.04$  and  $474.38\text{ cm}^{-1}$  illustrate the (Si-O-Si) group stretching (13, 14).

Figure 3 shows the spectra of XRD (X-ray Diffractometer) analysis spectra to determine the adsorbent phases and crystal properties used in the adsorption of Telon blue AGLF. In XRD analysis, the presence of large-scale peaks in the structure of the NiO-based nanomaterial shows that the crystals are small or structurally irregular, or both are valid, as well as regions of amorphous structure on the material other than the crystal structure (15).

SEM analyses were carried out to investigate the surface properties before and after the adsorption of nanoparticle used in the adsorption of Telon blue AGLF. From the SEM images before and after adsorption (Fig.4), it is determined that caves, pores, and surfaces of NiO-based adsorbent covered by dye molecule and the surface have become smoother (16).

### **Investigation of the Effects of Adsorption Parameters on Colour Removal**

The batch experiments were classified into four parts. Firstly, the effect of solution pH was studied. 0.1 g of the adsorbent was loaded into 150 mL of 100 mg L<sup>-1</sup> dye solution and adjusted the pH among 2.0 to 10.0 and then horizontally shaken at 200 rpm. The sample was collected at a time interval of 5 to 180 min. Secondly, the effect of the initial dye concentration on adsorption experiments was performed. 0.1 g of the adsorbent was loaded into 100 ml of 25 to 2000 mg L<sup>-1</sup> dye solution and horizontally shaken at 200 rpm for 180 min. At the next step, a series of experiments were performed at a temperature range of 30-65°C to observe the effect of the temperature on the adsorption process and finally, experiments were carried out in which the amount of adsorbent changed between 0.1 and 3.0 g L<sup>-1</sup> to investigate the effect of adsorbent at the same contact time and stirring speed. A series of adsorption experiments were carried out at the intervals mentioned above to determine the optimum adsorption conditions for the highest removal. A series of adsorption experiments were conducted at the above-mentioned adsorption parameter ranges to determine the optimum adsorption conditions for the highest removal values.

In the adsorption of TB AGLF onto NiO-based nanomaterials, pH 2.0, initial TB AGLF concentration 100 mg L<sup>-1</sup>, temperature 30°C and adsorbent concentration 1.0 g L<sup>-1</sup> were determined as the optimum conditions in which the highest color removal was observed. The effects of the initial pH in dye removal from aqueous solution have been shown in Fig. 5. The decrease in the amount of removal % values and the amount of adsorbed TB AGLF per unit mass of adsorbent at equilibrium was detected by an increase in the initial pH value from 2.0 to 10.0. In a study conducted by Nateghi et al. (2017) the adsorption process using nickel oxide nanoparticles was investigated for wastewater treatment containing mono azo Orange II dye. The results of this study showed that 0.6 g/L nickel

oxide was considered as the optimum amount of adsorbent for complete removal under the condition of 50 mg L<sup>-1</sup> initial dye concentration, pH value 3 and agitator speed 100 rpm about 30 minutes. Also, they determined the optimum pH value as 3 similar to the work done by the research group.

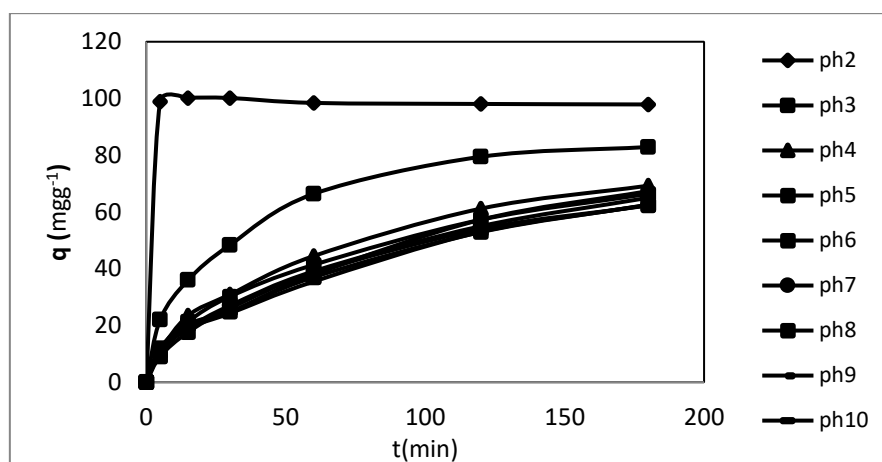


**Figure 5:** Effect of initial pH solution on the dye uptake on NiO-based nanomaterial.

According to the experimental results, pH 2 for the adsorption of Telon blue AGLF dye to NiO-based nanomaterials was determined as optimum value and adsorbed amount of dye per unit adsorbent mass and removal percentage were found as 97.9 mg/g and 96.15%, respectively at this value. At high pH values, the removal values were found to be low. Secondly, the effect of the initial dye concentration on adsorption experiments was performed. 0.1 g of the adsorbent was loaded into 100 mL of 25 to 2000 mg L<sup>-1</sup> dye solution and horizontally shaken at 200 rpm for 180 min.

At the next step, a series of experiments were performed at a temperature range of 30-65°C to observe the temperature effect on the adsorption process. From the experimental results, when the temperature increased from 30 °C to 60 °C, it was determined that the amounts of adsorbed dyes per unit mass of the adsorbent decrease significantly. For example, it was observed that the adsorbed dye amount at equilibrium decreased from 94.0 to 44.81 mg g<sup>-1</sup> when the temperature was increased from 30 °C to 60 °C at 100 mgL<sup>-1</sup>.

The initial dye concentration effect on the adsorbed amount of dye per unit mass of the NiO-based nanoparticle adsorbent was investigated between 25 and 2000 mg L<sup>-1</sup> at four different temperatures (30, 40, 50, 60 °C). Table 1 presents the adsorbed amount of Telon Blue AGLF per unit adsorbent mass and removal % values at the end of 180 min contact

time and the temperature of 30°C for the adsorption by NiO-based nanomaterials.

**Table 1:** The adsorbed amount of Telon Blue AGLF per unit adsorbent mass and removal % values at the end of 180 min contact time and at 30°C.

$C_0$ (mg L <sup>-1</sup> )	$q_d$ (mg g <sup>-1</sup> )	Removal %
22.72	21.62	95.15
41.81	40.45	96.73
61.90	60.45	97.65
98.18	94.00	95.74
190.9	187.0	97.95
318.1	314.4	98.82
397.2	390.0	98.16
529.0	521.8	98.62
737.2	729.5	98.95
1176.3	1034.5	87.94
1500.0	1307.2	87.15
1836.3	1412.7	76.93

As it seen from Table 1, the equilibrium sorption capacity of nanomaterial for dye increased notably with increasing initial dye concentration up to 2000 mg L<sup>-1</sup>. A similar result has been observed in other working temperatures. Kulkarni et al.(2016) investigated the effect of contact time, adsorbent dosage, adsorbate concentration and pH on Methylene Blue adsorption by ZnO particles. They found that at 180 min contact time equilibrium was achieved, 0.1 gm of ZnO loading and 100 ppm dye concentration and 6.5 pH conditions showed highest removal efficiency. According to the experimental results, it is clear that adsorbed amount of dye increases with increasing initial dye concentration from 25 mg L<sup>-1</sup> to 100 mg L<sup>-1</sup>, consistent with the results of our investigation.

In order to determine adsorbent dose effect on TB AGLF adsorption, a series of experiment were conducted at different adsorbent doses (0.50, 1.0, 2.0, 3.0 g L<sup>-1</sup>) for the initial dye concentration of 100 mg L<sup>-1</sup> at 30 °C and pH 2.0.

**Table 2:** The amount of adsorbed TB AGLF per unit mass of dye and removal % values.

$X_0$ (g L <sup>-1</sup> )	$q$ (mg g <sup>-1</sup> )	Removal %
0.1	626.3	68.62
0.5	146.1	72.82
1.0	94.00	95.91
2.0	34.04	82.57
3.0	25.09	90.47

From the experimental results, the increase in the removal % values with the adsorbent amount can be explained by the growth of the adsorbent surface area contacts with the dyestuff molecules. On the other hand, a reduction in the total surface area of the adsorbent as a result of the interaction and coagulation of the adsorbent particles can be claimed as the main reason for the decrease in adsorbed amount of dye by increasing amount of adsorbent.



### Equilibrium, Kinetic, and Thermodynamic Analysis

Adsorption isotherms provide some insight for the adsorption mechanism, the surface properties and affinity of the adsorbent for adsorbate. These models describe the nature of the interaction between adsorbate and the adsorbent used for the removal of different type of pollutants. The relevant information on the surface properties of the adsorbent and its affinity for the adsorbate were provided by the different isotherm model parameters. In this study, Langmuir and Freundlich's isotherms were chosen in order to analyze the Telon Blue AGLF adsorption by NiO-based nanomaterial. The best known of all isotherms describing adsorption is Langmuir adsorption isotherm (19). The following equation expresses the theoretical Langmuir isotherm:

$$q_d = \frac{Q^0 \cdot b \cdot C_d}{1 + b \cdot C_d} \quad (\text{Eq. 1})$$

where  $q_e$  is the equilibrium adsorption capacity ( $\text{mg g}^{-1}$ ),  $C_e$  is the equilibrium liquid phase concentration ( $\text{mg L}^{-1}$ ),  $Q^0$  is the maximum adsorption capacity, ( $\text{mg g}^{-1}$ ),  $b$  is adsorption equilibrium constant, ( $\text{L mg}^{-1}$ ).

The Freundlich isotherm is the earliest known relationship describing the adsorption isotherm (20). The Freundlich isotherm the earliest known relationship describing the adsorption isotherm can be used in adsorption from dilute solutions. The following equation expresses this adsorption isotherm:

$$q_d = K_f \cdot C_d^{(1/n)} \quad (\text{Eq. 2})$$

where  $C_e$  is dye concentration in the solution ( $\text{mg L}^{-1}$ ),  $q_e$  is the equilibrium adsorption capacity ( $\text{mg g}^{-1}$ ),  $K_F$  ( $(\text{mg g}^{-1})(\text{L/mg})^{1/n}$ ), and  $1/n$  are empirical constants.  $K_F$  is the adsorption value, the amount adsorbed at unit concentration, that is, at  $1 \text{ mg L}^{-1}$ .  $n$  is the density of adsorption.

Temkin isotherm model is found by assuming that the decrease in adsorption energy is not exponential but linear as in the Freundlich equation. The following formula expresses this adsorption isotherm:

$$q_d = \frac{R \cdot T}{b} \cdot \ln(A_t \cdot C_d) \quad (\text{Eq. 3})$$

where  $b$  is the model constant about adsorption heat ( $\text{J mol}^{-1}$ ),  $R$  is Ideal gas constant ( $8,314 \text{ J mol}^{-1} \text{ K}^{-1}$ ),  $A_t$  is Temkin isotherm constant ( $\text{L g}^{-1}$ ) and  $T$  is temperature (K).

Freundlich and Temkin isotherm model graphs representing the experimental data are given in Fig.7 and Fig. 8.

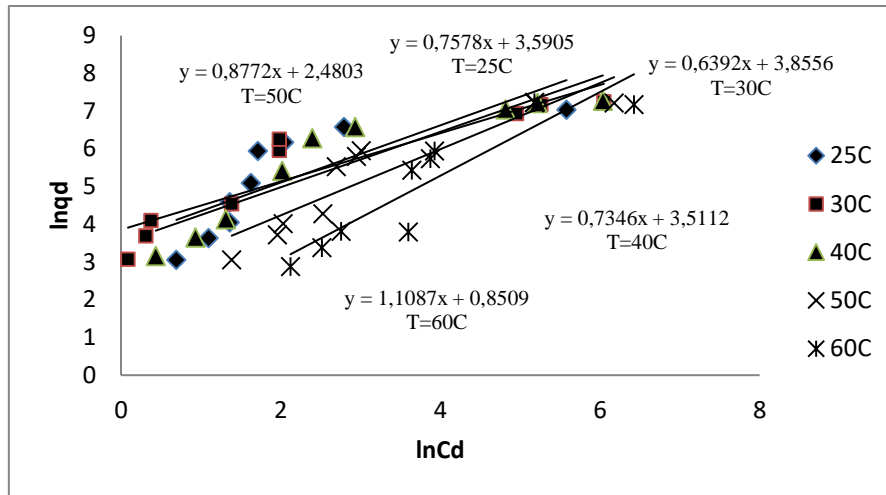


**Figure 6:** Freundlich isotherm curves obtained for the adsorption of Telon blue AGLF dye onto NiO-based nanomaterials.

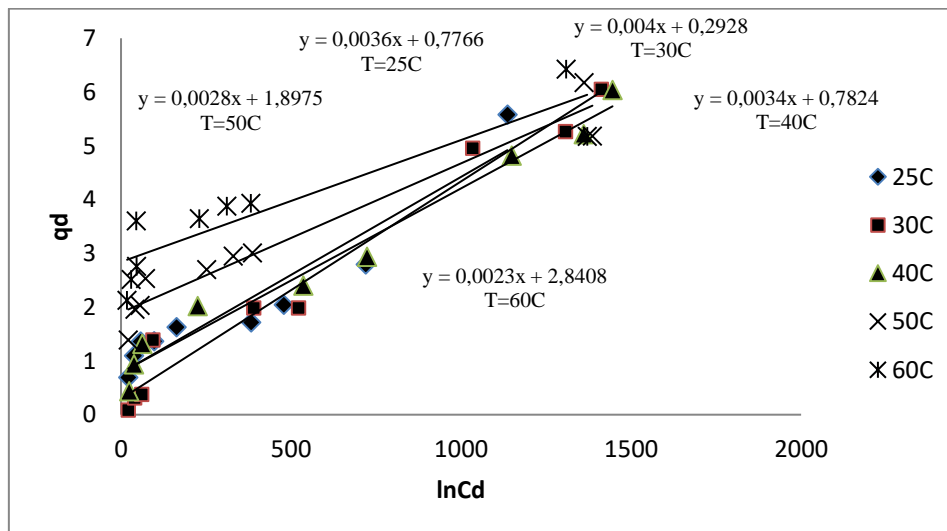


**Figure 7:** Temkin isotherm curves obtained for the adsorption of Telon blue AGLF dye onto NiO-based nanomaterials

In this part, firstly, the compatibility of the adsorption equilibrium data with Langmuir-Freundlich and Temkin isotherm models were evaluated, and the results were presented in Table 1 in order to find the best model represents the equilibrium data for TB AGLF adsorption onto nanomaterials. Despite the high correlation coefficients in Langmuir model, the negative slope and the negative Langmuir isotherm constants resulting from the model calculations indicate that this model is inadequate to explain this adsorption process. In Freundlich isotherm model,  $n$  values calculated at different temperatures are greater than 1 or equal to 1 indicate that NiO-based nanoparticles used in the adsorption process are favorable adsorbents. Accordingly, it is detected that the adsorption characteristic can be represented by the Freundlich model. According to Table 3, it is seen that the values of the

correlation coefficients for Temkin isotherm are higher than those of Langmuir and Freundlich isotherm constants. So the adsorption characteristic can be best represented by Temkin model.

**Table 3:** Langmuir, Freundlich and Temkin Isotherm model constants for TB AGLF adsorption.

<b>Langmuir Model Constants</b>					
Temperatures	T=25°C	T=30°C	T=40°C	T=50°C	T=60°C
Q <sup>o</sup> (mg/g)	-123.46	-833.33	-714.28	-250.00	370.37
b (L/mg)	-0.0833	-0.0297	-0.0210	-0.0208	0.0255
R <sup>2</sup>	0.868	0.872	0.983	0.946	0.956
R <sub>L</sub>	-0.136	-0.507	-0.909	-0.925	-0.645
<b>Freundlich Model Constants</b>					
Temperatures	T=25°C	T=30°C	T=40°C	T=50°C	T=60°C
1/n	0.75	0.64	0.735	0.88	1.11
n	1.32	1.56	1.36	1.13	0.90
K <sub>f</sub>	36.23	47.25	33.48	11.94	2.34
[(mg/g)/(L/mg) <sup>1/n</sup> ]					
R <sup>2</sup>	0.631	0.851	0.838	0.831	0.835
<b>Temkin Model Constants</b>					
Temperatures	T=25°C	T=30°C	T=40°C	T=50°C	T=60°C
<b>A<sub>t</sub> (L/g)</b>	<b>0.522</b>	<b>0.792</b>	<b>0.735</b>	<b>0.88</b>	<b>1.11</b>
<b>B (J/mol)</b>	249.08	180.5	1.36	1.13	0.90
<b>R<sup>2</sup></b>	0.908	0.973	0.974	0.943	0.833

Kinetic models investigated the mechanism of sorption and potential rate controlling steps, which is helpful for selecting optimum operating conditions. There are two commonly used kinetic models in mechanism investigations. In order to analyze the adsorption kinetics of TB AGLF onto NiO-based nanomaterials, compatibility of pseudo first-order and pseudo second order kinetic models with the experimental data was investigated. The pseudo-first-order rate expression (19) is expressed as follows Eq (3) and (4), respectively:

$$dq_t/dt = k_1(q_e - q_t) \quad (\text{Eq. 3})$$

where  $q_e$  is the amount of dye adsorbed at equilibrium (mg/g),  $q_t$  is the amount adsorbed at time  $t$  (mg g<sup>-1</sup>),  $k_1$  is the rate constant of first-order adsorption (min<sup>-1</sup>).

with the application of integration and boundary conditions,  $t=0$  to  $t$  and  $q_t=0$  to  $q_e$ ; the form of equation (3) becomes:

$$\log (q_e - q_t) = \log q_e - k_1 t / 2.303 \quad (\text{Eq. 4})$$

By plotting  $(q_e - q_t)$  values versus  $t$  the value of adsorption rate constant  $k_1$  for the adsorption was determined.

The pseudo second order rate equation (21) is expressed by the following formula:

$$dq_t/dt = k_2(q_e - q_t) \tag{Eq. 5}$$

Where  $k_2$  is the rate constant of second order-adsorption (g/mg.min).

For the same boundary conditions the integrated form of equation (5) becomes:

$$t/q_t = 1/k_2q_e^2 + t/q_e \tag{Eq. 6}$$

where  $k_2$  was determined from the slope and intercept of the plots of  $t/q$  against  $t$ .

The graphs of first and second-order kinetic model for adsorption of telon blue AGLF on NiO-based nanomaterial are presented in Figures 7 and 8 respectively.

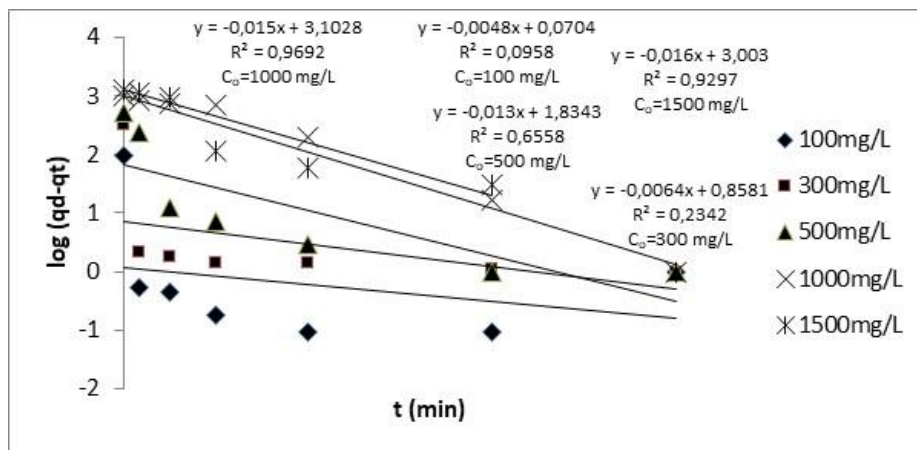


**Figure 8:** The graph of pseudo-first order kinetic model for TB AGLF adsorption by NiO-based nanomaterials.

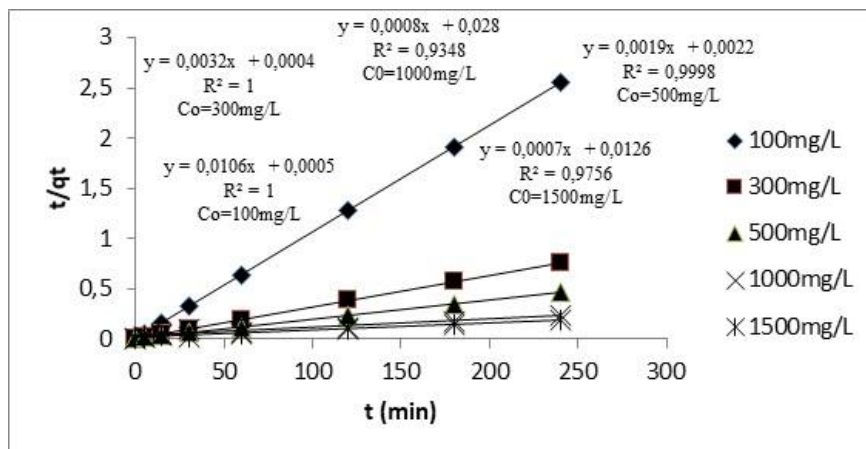


**Figure 9:** The graph of pseudo first, second kinetic model for TB AGLF adsorption by NiO-based nanomaterials.

The constants obtained by plotting the linear forms of the models with the regression coefficients for both models are shown in Table 4. When Table 4 is evaluated, too low regression coefficients of the pseudo first-order kinetic model indicate that the first-order kinetic equation can not be applied to the experimental data.

It can be shown that both the regression coefficients for the equations are high and the equilibrium data calculated experimentally and theoretically are closer to each other, so this phenomenon is a sign of better adaptation of the second order kinetic model to the adsorption process. The appropriate (close to 1) values of the regression coefficients and approximately equal experimental and calculated theoretical values are evidence of better compatibility of the second order kinetic model for the adsorption process.

**Table 4:** Pseudo first and second order model rate constants and regression coefficients values for TB AGLF adsorption.

$C_0$ (mg L <sup>-1</sup> )	Pseudo first order model		Pseudo second order model	
	$K_1$ (min)	$R^2$	$K_2$ (g/mg.min)	$R^2$
25	0.0170	0.423	0.0293	0.999
50	0.0258	0.474	0.0484	1.000
75	0.0143	0.356	0.0377	1.000
100	0.0113	0.095	0.2250	1.000
200	0.0212	0.403	0.0468	1.000
300	0.0147	0.234	0.0256	1.000
400	0.022	0.420	0.0169	1.000
500	0.030	0.655	0.0016	0.991
750	0.055	0.739	0.0060	0.998
1000	0.034	0.021	0.0005	0.999
1500	0.0037	0.929	3.89E-05	0.975

At the next stage, thermodynamic parameters of the system were determined by Van't Hoff equation, and the values obtained from this equation are presented in Table 5. According to Table 5, it is determined that adsorption onto NiO-based nanomaterial is endothermic ( $\Delta H > 0$ ), stable without structural change at the solid/liquid interface (low  $\Delta S$  value), and a spontaneous ( $\Delta G < 0$ ).

**Table 5:** Thermodynamic parameters for TB AGLF adsorption.

T(K)	$\Delta G$ (J mol <sup>-1</sup> )	$\Delta H$ (J/mol)	$\Delta S$ (J/ mol <sup>-1</sup> K <sup>-1</sup> )	$T\Delta S$ (J mol <sup>-1</sup> )
298	-3602.75			15416.7
303	-4822.70	11284.6	51.73	15675.4
313	-5198.82			16192.7
323	-5509.51			16710.0

According to the experimental results, as the temperature increases in the adsorption system, the enthalpy values have a positive sign despite the decrease in color removal yield at a forward direction of the adsorption process. This phenomenon is explained in the literature as follows: at high temperatures where both  $\Delta H$  and  $\Delta S$  are positive ( $T\Delta S > \Delta H$ ),  $\Delta G$  values always have a minus sign (22, 23).

## CONCLUSION

In this study, color removal was investigated by using NiO-based nanomaterials from synthetic wastewaters containing TB AGLF dye, and it was observed that high yield (%95.74-%76.93 at  $T=30$  °C and the TB AGLF concentration range of 25-2000 mg L<sup>-1</sup>) color removal was achieved with synthesized nanomaterial. For the future work, studies on the design of real wastewater treatment systems containing more than one pollutant at high concentrations can be carried out using the balance, kinetic and thermodynamic analysis results obtained in this laboratory experiments.

The most significant contribution of this investigation to the world and our country is to prove the sustainability of scientific researches in accordance with the economically and the efficient treatment processes about the recovery of the polluted water resources.

## REFERENCES

1. Wang S and Li H. Dye adsorption on unburned carbon: Kinetics and equilibrium. *Journal of Hazardous Materials*. 2005;126:71–77.
2. Gregory AR, Elliot, J, Kluge P. Ames testing of direct black 38 parallels carcinogenicity testing. *Journal of Applied Toxicology*. 1981;1:308–313.
3. Gong R, Ding Y, Li M, Yang, C, Liu H, Sun Y. Utilization of powdered peanut hull as biosorbent for removal of anionic dyes from aqueous solution. *Dyes and Pigments*. 2005;64(3):187–192.
4. Ejhieh AN and Khorsandi, M, Photodecolourization of Eriochrome Black T using NiS-P zeolite as a heterogeneous catalyst. *Journal of Hazardous Materials*. 2010;176:629-637.
5. Riyanto E, Norazizi N, Mohamed RO. Textiles Industries Wastewater Treatment by Electrochemical Oxidation Technique using Metal Plate. *International Journal of Electrochemical Science*. 2013;8:11403-11415.
6. Vucurovic VM, Razmovski RN, Miljic UD, Puskas VS. Removal of cationic and anionic azo dyes from aqueous solutions by adsorption on maize stem tissue. *Journal of the Taiwan Institute of Chemical Engineers*. 2014;45:1700–1708.
7. Nemr AE, Abdelwahab O, El-Sikaily A, Khaled A. Removal of direct blue-86 from aqueous solution by new activated carbon developed from orange peel. *Journal of Hazardous Materials*. 2009;161(1),102–110.
8. Crini G, Non-conventional low-cost adsorbents for dye removal: A review, *Bioresour. Technol*. 2006; 97: 1061– 1085.
9. Schmid G. Large clusters and colloids—metals in the embryonic state. *Chem Rev* . 1992;

92:1709–1727.

10. Andres RP, Bielefeld JD, Henderson JI, Janes DB, Kolagunta VR, Kubiak CP, Mahoney WJ, Osifchin RG. Self-assembly of two-dimensional superlattice of molecularly linked metal clusters. *Science*, 1996; 273:1690–1693

11. Sheshdeh RK, Khosravi, MR Nikou, Badii K, Limaee NY, Golkarnarenji . Equilibrium and kinetics studies for the adsorption of Basic Red 46 on nickel oxide nanoparticles-modified diatomite in aqueous solutions. *Journal of the Taiwan Institute of Chemical Engineers*. 2014;45:1792–1802.

12. Uzunoğlu D, Özer A, Uslu A, Elbağlı O, Şen Y. The Investigation of the Adsorption of Acid Blue 121 on Banana Shell in a Batch System *Anadolu Üniversitesi Bilim Ve Teknoloji Dergisi A*, 2015;16(2):293-302.

13. Chowdhury AN, Rahim, A, Ferdosi YJ, Azam, MS, Hossain, MM. Cobalt–nickel mixed oxide surface: A promising adsorbent for the removal of PR dye from water, *Applied Surface Science*, 2010;256: 3718–3724.

14. Gabrovska M, Krstić J, Edreva-Kardjieva, R, Stanković M, Jovanović D. The influence of the support on the properties of nickel catalysts for edible oil hydrogenation. *Applied Catalysis A: General*. 2006;299:73–83.

15. Uzunoğlu D, Özer A. Levrek Balığı (*Dicentrarchus Labrax*) Pulu Ve Ticari Hidroksiapatit ile Acid Blue 121 Boyarmaddesinin Adsorpsiyonu. Yüksek Lisans Tezi, Mersin Üniversitesi Fen Bilimleri Enstitüsü, Mersin, 2014.

16. Vijayakumar G, Tamilarasan R, Dharmendirakumar M. Adsorption, Kinetic, Equilibrium and Thermodynamic studies on the removal of basic dye Rhodamine-B from aqueous solution by the use of natural adsorbent perlite. *J. Mater. Environ. Sci.* 2012;3(1):157-170.

17. Nateghi R, Bonyadinejad GR, Amin MM, Mohammadi H. Decolorization of synthetic wastewaters by nickel oxide nanoparticle. *Int J Env Health Eng* 2012;1-25

18. Kulkarni AV, Chavhan A, Bappakhane A, Chimankar ZnO Nanoparticles as Adsorbent for Removal of Methylene Blue dye. *J. Res J. Chem. Environ. Sci.* Vol 4 [4S] 2016: 158-163

19. Langmuir I. The adsorption of gases on plane surfaces of glass, mica and platinum. *J. Am. Chem. Soc.* 1918;40:1361-1403.

20. Freundlich, H.M.F. Über die Adsorption in Lösungen. *Z. Phys. Chem-Leipzig*. 1906; 57A, 385-470.

21. Chang R. Fen ve Mühendislik Bölümleri İçin Kimya. İstanbul: Beta Basım Yayım Dağıtım A.Ş.;2000.

22. Mortimer CE. Chemistry-A conceptual Approach. Van Nostrand, New York;1979.

23. Meroufel B, Benali O, Benyahia M, Benmoussa Y, Zenasni MA. Adsorptive removal of anionic dye from aqueous solutions by Algerian kaolin: Characteristics, isotherm, kinetic and thermodynamic studies . *J. Mater. Environ. Sci.* 2013; 4 (3): 482-491.

